COMMISSIONING OF THE SPARC PHOTO-INJECTOR*

M. Bellaveglia, D. Alesini, S. Bertolucci, M. E. Biagini, R. Boni, M. Boscolo,
M. Castellano, E. Chiadroni, A. Clozza, L. Cultrera, G. Di Pirro, A. Drago, A. Esposito,
M. Ferrario, L. Ficcadenti, D. Filippetto, V. Fusco, G. Gatti, A. Gallo, A. Ghigo,
S. Guiducci, M. Incurvati, C. Ligi, M. Migliorati, A. Mostacci, L. Palumbo,
L. Pellegrino, M. Preger, R. Ricci, C. Sanelli, F. Sgamma, B. Spataro,
F. Tazzioli, C. Vaccarezza, M. Vescovi, C. Vicario (INFN/LNF);
A. Bacci, I. Boscolo, F. Broggi, S. Cialdi, D. Giove, M. Mauri,
A. Rossi, L. Serafini (INFN/Milano);
M. Mattioli, P. Musumeci, M. Petrarca (INFN/Roma1);
L. Catani, A. Cianchi, S. Tazzari (INFN/Roma2);
A. Perrone (INFN /Lecce);
L. Giannessi, M. Quattromini, A. Renieri, C. Ronsivalle (ENEA/FIS);
J. Rosenzweig (UCLA)

Abstract

The SPARC project [1] is born to perform R&D activity headed to realize SASE-FEL experiments at $500nm$ and higher harmonic generation. The project foresees the realization of a high brightness photo-injector able to produce a $150 \div 200MeV$ electron beam to drive FEL process inside a dedicated $12m$ long undulator. The machine is going to be assembled at LNF and its final configuration is made up of an RF gun, driven by a Ti:Sa laser, injecting into three SLAC type accelerating sections. Nowadays we are working in a photo-injector test phase, aiming to characterize the main hardware components and to investigate the behavior of the e-beam dynamics in the first meters of drift. To do this we utilize the emittance-meter, a home designed diagnostic device placed just after the RF gun, able to move 1.2 meters along the longitudinal axis to measure beam parameters. In this paper we report a more accurate description of the project, the status of the single systems constituting the machine and the most important results we obtained in the e-meter phase.

INTRODUCTION

The commissioning of the SPARC photo-injector is started at Frascati INFN laboratories and we are operating in a gun test phase, before installing the accelerating sections. In this phase, laser, radiofrequency, timing, control system and beam diagnostics are installed and working in the SPARC bunker. We performed a characterization of the beam at the gun exit with the home-designed movable emittance-meter [2] and a spectrometer. A picture of the hardware installed in the bunker is reported in figure 1. The most significant results are reported in table 1 that shows the two investigated main beam configurations.

Table 1: Main beam configurations

	Low charge	High charge
Charge	$200pC$	$900pC$
Emittance	$0.8mm\ mrad$	$2.2mm\ mrad$
Energy	$5.65MeV$	$5.55MeV$
Energy spread	1%	2.6%
Pulse length	$8ps$	$12ps$

PHOTO-INJECTOR STATUS

In the following paragraphs we will give a short description of the main systems constituting the machine.

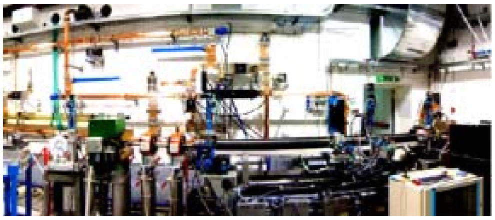

Figure 1: Picture taken in the SPARC bunker

RF and timing system

The SPARC RF system is mainly constituted by two RF chains and its scheme is reported in figure 2 together with the synchronization system layout [3]. The power sources, shown in figure 3(a), are the 45 MW peak, 2856 MHz klystrons TH2128C. The klystron n.1 presently feeds only the RF gun with $3\mu sec$ pulses and it is designed to feed also one accelerating section via a $3dB$ waveguide coupler and an RF deflecting cavity for beam diagnostic purposes.

The RF gun, reported in figure 3(b), was successfully conditioned without relevant problems and we fed into it more than $10MW$ of RF power that corresponds to an

---

* Work supported by the EU Commission in the 6th FP, contract no. 011935 EUROFEL and contract no. RII3-CT-2003-506395 CARE.

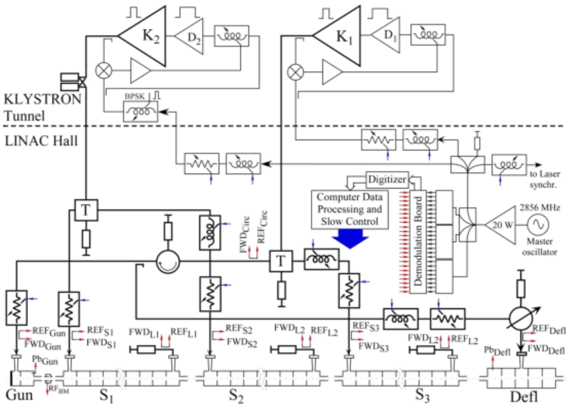

Figure 2: RF system layout

(a) (b)

Figure 3: Installed RF hardware: (a) modulators and klystrons and (b) RF gun

accelerating electric field of about $120MV/m$. Klystron n. 2 and its waveguide distribution lines are now under test and they will feed two high gradient accelerating sections through an energy compressor that allows to obtain a $60MW$ - $0.8\mu sec$ RF pulse.

The timing distribution system is installed and it provides the $79.33MHz$ reference to lock the laser system to the RF oscillator using a home-designed frequency divider board. It also furnish the $10Hz$ repetition rate signal to the machine, synchronous with the external line and to the $2856MHz$ internal distribution.

The synchronization diagnostic is working with good and stable performances and the time jitter from each location of the machine (relative to the main oscillator) is displayed in the control room monitors. Also an RF phase feedback system was implemented to correct slow drifts due to temperature. The observed time jitter of the accelerating field inside the gun is $250fs_{RMS}$ and the laser oscillator time jitter is $350fs_{RMS}$.

Laser system

Beam dynamics simulations defined the SPARC laser system [4] specs in order to obtain $2mm\ mrad$ emittance at $100A$. The laser is a $10Hz$ CPA Ti:SA, TW system produced by Coherent. At the laser exit a THG and an UV stretcher produce the required wavelength ($266nm$) and pulse duration ($2 \div 10ps$). To manipulate the time profile an acousto-optic programmable dispersive filter is installed before the amplifier.

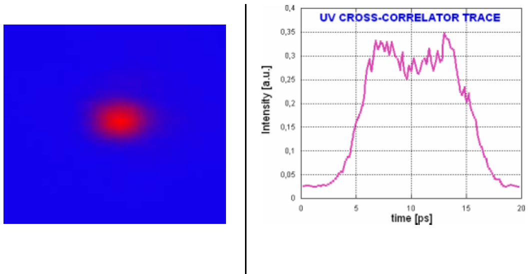

(a) (b)

Figure 4: (a) transverse laser spot on the cathode and (b) UV pulse longitudinal shape

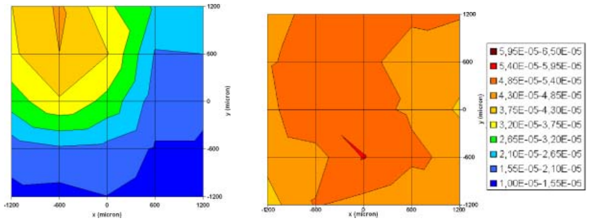

Figure 5: Cathode QE before (left) and after (right) laser cleaning

The pulse profile is flat in time and gaussian in transverse plane (with $1mm$ spot size) and an image of the spot is shown in figure 4(a). We are using a cross-correlator to investigate the longitudinal behavior of the UV pulse and a typical observed shape is reported in figure 4(b). The optical transfer line is designed to increase the pointing stability, to easily change the spot dimension and to compensate the 72° incidence distortions.

A laser cleaning on the cathode was performed and it has given good results, increasing the quantum efficiency from $3.75 \cdot 10^{-5}$ to $6 \cdot 10{-}5$ and improving the emission uniformity as can be seen in figure 5.

Control system

The control system is perfectly working and it is ready to be extended to the SPARC full configuration. The SPARC main server with a RHEL3 operating system, is in a LTSP configuration so that the consoles are identical diskless workstations. The photo-injector device drivers are installed in industrial PCs placed in the bunker. The layout of figure 6 report the SPARC protected $1Gbit/s$ LAN architecture. Two machines form a connecting bridge from the front-end industrial PCs to the control room consoles:

- the data server: it accepts a request of information from the consoles and send them the data read from the proper industrial PC. The data can be software variables (that identify the controlled devices), sampled signals, images or information about the status of the computer itself;

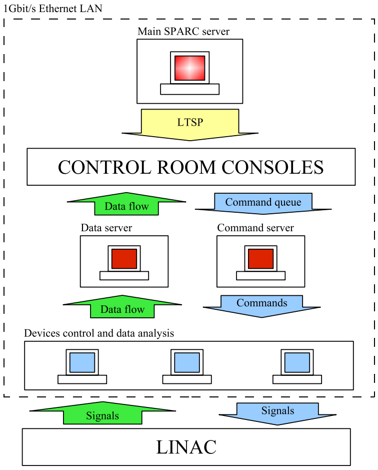

Figure 6: Control system architecture

- the command server: it elaborates the queue coming from the consoles and, once identified legal commands, it delivers them to the front-end PCs to control the photo-injector devices.

Diagnostics

Beam diagnostic devices are placed along the photo-injector as shown in figure 7 and reported in table 2. The main diagnostic tool is the home-designed emittance-meter, able to move $1.2m$ along the longitudinal axis and to study the first meters of beam propagation, where space charge effects and plasma oscillations dominate the electron dynamics.

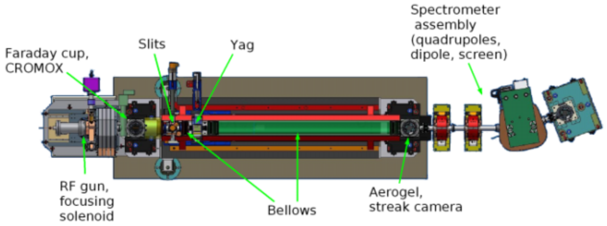

Figure 7: Photo-injector actual layout

Table 2: Diagnostic elements

Distance from cathode [cm]	Device	Measurement
60	Faraday cup, CROMOX screen	charge, beam centering
$85 \div 200$	E-meter (slits, YAG screen, CCD)	emittance, beam envelope and parameters
220	aerogel + streak camera	beam duration
$250 \div 300$	FODO cell, dipole	beam conditioning before spectrometer
$250 \div 300$	spectrometer (Yag + CCD)	energy and energy spread
350	BCM	beam charge

An exhaustive description of the measurements taken using these items is given in the next section.

BEAM MEASUREMENTS

Charge vs phase

First of all we report the charge relative to the gun RF phase measurement (phase scan) that allow us to choose day by day the optimal phase for the electron extraction and to collect information about the accelerating gradient and the quantum efficiency. Moreover this kind of measurement permit us to obtain a rough estimation of the beam duration. Picture 8 report some phase scans performed in different photo-injector working points.

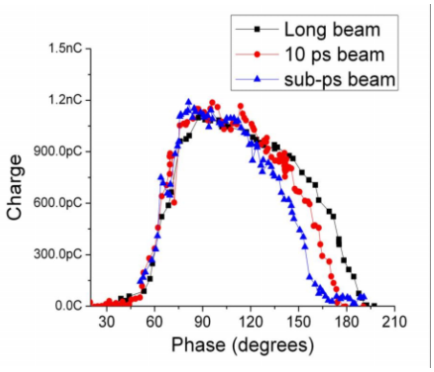

Figure 8: Charge vs phase in three different beam configurations

Energy and energy spread

A spectrometer and its transport line (constituted by a FODO cell) are placed at the end of the diagnostics chain to measure energy and energy spread. We performed these measurements in low and high charge configurations as function of the launching phase as shown in figure 9. The difference both in maximum energy and energy spread between the low and high charge case are due to longitudinal space charge effects (including the image charge at the cathode) and to the wakefield effects in the long bellows.

The presence of the emittance-meter allowed us to perform some special energy spread measurements inserting a slit in the bunch orbit and selecting a beam slice in different longitudinal locations. In fact, as shown in picture 10, we ‘froze’ the beam evolution under the longitudinal space charge and wakefield effects at different points along the beamline.

Bunch length

A longitudinal diagnostic, based on Cherenkov radiation produced by the beam passing through a $5mm$ thick aerogel slab with index of refraction $n = 1.017$, was installed with the main purpose of studying the photo-injector response to hundreds femtosecond long laser pulses created

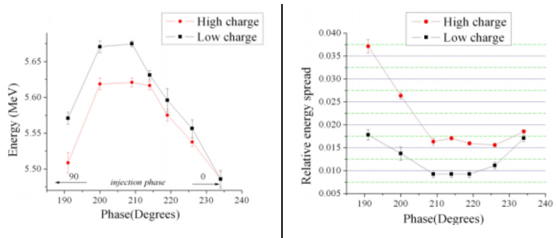

(a) (b)

Figure 9: Energy (a) and energy spread (b) for low and high bunch charge

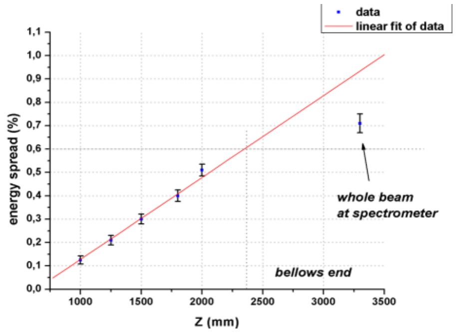

Figure 10: 'Slit' energy spread

by the Ti:Sa laser system [5]. A field-lens narrow band filtering optical system delivers the Cherenkov light to the entrance slit of a $2ps$ resolution Hamamatsu streak camera enabling pulse length measurements (see figure 11).

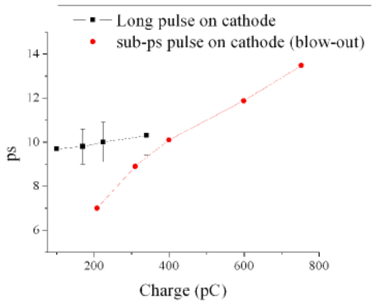

Figure 11: Bunch length measurements with streak camera

Transverse dynamics

Using the emittance-meter we were able to characterize the emittance as function of the longitudinal coordinate and to observe clear indications of emittance oscillations driven by space charge forces in the drift downstream of the RF gun, in agreement to what expected from our theoretical model and numerical simulations. Figure 12 reports two set of measurements compared with numerical simulation. The algorithm used to calculate the emittance was designed also to reconstruct the phase space and good results were achieved (see figure 13).

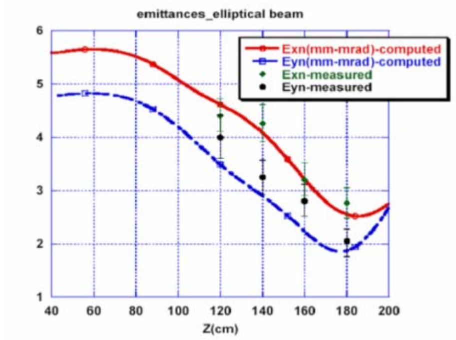

Figure 12: Emittance measurement with relative simulated curves

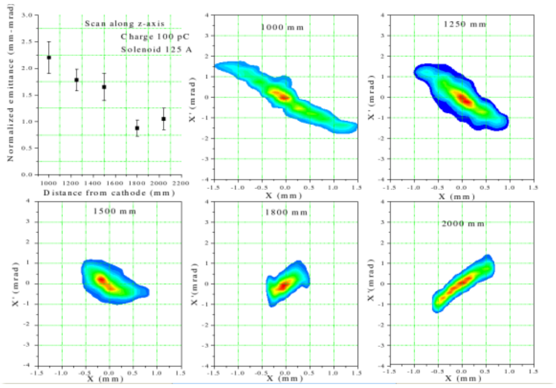

Figure 13: Phase space reconstruction

CONCLUSIONS

The SPARC photo-injector commissioning was started and a good characterization of the electron beam at the exit of the gun has been performed with the emittance-meter. In particular measurements show that the beam brightness required to drive a SASE-FEL experiment was achieved. The linac installation phase will begin at the end of this summer with the commissioning of the accelerating sections and the second RF power line. Moreover it is planned to use a SPARC-like system as photo-injector for the future SPARX X-ray FEL experiment [6].

REFERENCES

[1] D.Alesini et al., IEEE Cat. N. 05CH37623C, (2005) 1327.

[2] L. Catani et al., 'Operational experience with the emittance-meter at SPARC', these proceedings.

[3] A. Gallo et al., 'The SPARC RF Synchronization System', PAC'05 proceedings, Knoxville, May 2005, p. 1024.

[4] C. Vicario et al., 'Commissioning of the Laser System for SPARC Photoinjector', EPAC'06 proceedings, Edinburgh, June 2006.

[5] M. P. Dunning et al., 'Optimum beam creation in photoinjectors using space-charge expansion', these proceedings.

[6] D. Alesini et al., 'Status of the SPARX FEL project', EPAC'06 proceedings, Edinburgh, June 2006.